Earth and Space Science

RESEARCH ARTICLE
10.1029/2019EA001052

Quantification of Uncertainty in Projections of Extreme Daily Precipitation

Seokhyeon Kim[1], Sajjad Eghdamirad[2], Ashish Sharma[1], and Joong Hoon Kim[2]

[1]School of Civil and Environmental Engineering, University of New South Wales, Sydney, New South Wales, Australia, [2]School of Civil, Environmental, and Architectural Engineering, Korea University, Seoul, South Korea

Key Points:
- Uncertainty in projected extreme precipitation is ascertained and attributed to source using the square root error variance (SREV) metric
- Higher relative uncertainty is found for dry regions compared to wet regions
- Higher scenario and ensemble uncertainty is found in maximum daily precipitation projections compared to average precipitation

Supporting Information:
- Supporting Information S1

Correspondence to:
J. H. Kim,
jaykim@korea.ac.kr

Citation:
Kim, S., Eghdamirad, S., Sharma, A., & Kim, J. H. (2020). Quantification of uncertainty in projections of extreme daily precipitation. *Earth and Space Science*, *7*, e2019EA001052. https://doi.org/10.1029/2019EA001052

Received 12 DEC 2019
Accepted 7 JUL 2020

Abstract Projections of extreme precipitation are of considerable interest in a range of design and management applications. These projections, however, can exhibit uncertainty that requires quantification to provide confidence to any application they are used in. This study assesses the uncertainty in projected extreme daily precipitation, separated into model, scenario, and ensemble components using the square root error variance (SREV) rationale. For this, 45 projections of daily precipitation from the Coupled Model Intercomparison Project Phase 5 (CMIP5) are used, consisting of multiple global circulation models and their ensemble members, for a range of Representative Concentration Pathways, allowing assessment across land-covered areas worldwide. It is found that the uncertainty in dry regions is significantly higher compared to wet regions, raising concerns regarding infrastructure design for the future in arid parts of the world. It is also found that the climate scenarios and initialization contribute significantly to the overall uncertainty, compared to contributions for more nonextreme precipitation simulations. This finding has implications in how design precipitation extremes ought to be projected into the future, with greater attention being paid on a broader selection of emission scenarios and initializations than is the case with projections of nonextreme precipitations.

Plain Language Summary Projections of extreme precipitation are of considerable interest in a range of design and management problems. These projections, however, are subject to considerable uncertainty, which requires quantification before they can be put to use. This study quantifies the uncertainty in projected daily extreme precipitations worldwide and attributes this uncertainty into distinct dominant sources using a range of extreme daily precipitation simulations from the Coupled Model Intercomparison Project Phase 5 (CMIP5). The results indicate that extreme precipitation exhibits greater uncertainty in dry regions, such as North Africa and the Middle East, compared to wetter regions. Results also indicate that emission scenarios and model initializations strongly contribute to the uncertainty in the maximum extreme precipitation, more so than for nonextreme precipitation.

1. Introduction

Quantifying climate change impact on the global water cycle is an important challenge for multiple sectors, including the environment, economy, and agriculture (Hegerl et al., 2015; Marotzke et al., 2017). It is widely accepted that water security will worsen, both in terms of flood impact and water supply security, as temperatures rise beyond 3.5°C (IPCC, 2014; Kundzewicz et al., 2008; Miller & Yates, 2006; Peters et al., 2012; Sharma et al., 2018). The Coupled Model Intercomparison Project Phase 5 (CMIP5) has provided multiple projections of likely future climates based on Global Circulation Model (GCM) simulations using Representative Concentration Pathways (RCP) and multiple ensemble members representing the impact of model initializations (Van Vuuren et al., 2011). Such GCM projections have been widely used to understand which policies and strategies can be adopted to mitigate the negative impacts of a warmer climate (IPCC, 2014; Meinshausen et al., 2009; Schleussner et al., 2016; Vermeulen et al., 2012). In spite of their usefulness, these GCM outcomes exhibit high uncertainty as a result of many factors including imperfect representation of the climate system, assumed greenhouse gas emission scenarios, limited spatial and temporal resolution, and errors in the forcing data (Murphy et al., 2004; Randall et al., 2007; Stainforth et al., 2005).

To assess the impact of this uncertainty in future projections, several qualitative and quantitative assessments have been attempted at monthly, seasonal, annual, and decadal time scales. Hawkins and Sutton (2009) introduced disagreement among GCM projections as a measure of uncertainty for climate

variables. Hawkins and Sutton (2009, 2011) and Yip et al. (2011) quantified the uncertainty in mean annual temperature and precipitation projections by disaggregating uncertainty into three sources: model, scenario, and internal variabilities. Deser et al. (2012) highlighted that the natural (i.e., internal) variability plays an important role to regulate the predictability of future climate. Hayhoe et al. (2007) showed the importance of future emission scenarios in determining the potential magnitude of future climate changes. A new rank-based metric for quantifying uncertainty in monthly projections was presented in (S. Eghdamirad et al. (2016); F. M. Woldemeskel et al. (2012, 2014, 2016). The estimated uncertainty was then applied to compare the reliability of GCM monthly projections (Sajjad Eghdamirad et al., 2017) for use in hydrologic climate change impact assessment studies.

For future water planning, the ability of GCMs to accurately project daily precipitation is of concern (Hawkins & Sutton, 2011; Teng et al., 2012), and it is also important to ascertain how this uncertainty changes with time since long-term changes in precipitation are not monotonic (Hawkins et al., 2014). However, a majority of the approaches aim to ascertain overall or average uncertainty in the variable of interest, rather than how this uncertainty varies with magnitude, space, and time. Past attempts at quantifying uncertainty in future daily precipitation have been based on the disagreement between projections and observations of the present climate (Fischer et al., 2013, 2014; Fischer & Knutti, 2015; Kharin et al., 2013; Sillmann et al., 2013), thereby precluding uncertainty estimates as a function of time which allows focus on scenarios that can result in a failure of the system (such as flooding) these form inputs for.

While the uncertainty in daily precipitation is of interest, perhaps of greater interest is the uncertainty associated with daily precipitation extremes. This is because such extremes are often the key factor for infrastructure failure as a result of flooding, and hence associated uncertainty can complement derived estimation of design flood values or other applications where a design precipitation sequence becomes important. There is also considerable interest in changes in precipitation extremes due to rising temperatures, as more moisture is expected to be stored, and released, in a warmer atmosphere (L. V. Alexander & Arblaster, 2017; Hegerl et al., 2015; C. Wasko & Sharma, 2015; Conrad Wasko et al., 2015; Zarekarizi et al., 2018), leading many to speculate that at least urban stormwater infrastructure will be more prone to failure than before (K. Alexander et al., 2019; S. Hettiarachchi et al., 2018; Suresh Hettiarachchi et al., 2019).

To address the abovementioned limitations, this study attempts to quantify uncertainty in daily precipitation projections, with a focus on daily precipitation extremes. Uncertainty is attributed to three dominant sources, that is, model, scenario, and ensemble uncertainties. The present study also aims to provide a better understanding of regional climate change (Xie et al., 2015), by illustrating whether GCMs show a change in skill in projecting precipitation extremes across different parts of the world.

In this paper, section 2 presents a brief description of the data used in this study and procedures adopted to calculate uncertainty; the results and discussion are described in section 3, and the paper is summarized and concluded in section 4.

2. Data and Method

2.1. Data and Preprocessing

In the current study, a total of 45 projections of daily precipitation from the CMIP5 data depository over the period 2006–2100 were used. The 45 projections are combinations of five GCMs (i.e., CanESM2, CSIRO-MK3–6-0, HadGEM2-ES, IPSL-CM5A-LR, and MIROC5) listed in Table 1, three scenarios (RCP2.6, RCP4.5, and RCP8.5), and three ensembles (r1i1p1, r2i1p1, and r3i1p1).

RCPs 2.6, 4.5, and 8.5 represent “low,” “medium,” and “high” prescribed pathways for greenhouse gas and aerosol concentrations by 2100, characterized by the radiative forcing of 2.6, 4.5, and 8.5 W/m^2, respectively, and the CO_2-equivalent concentrations of 421, 538, and 936 ppm, respectively (Meinshausen et al., 2011). The ensemble members in CMIP5 follow the rip-nomenclature, *r* for realization, *i* for initialization, and *p* for physics, followed by an integer for each initialization (e.g., r1i1p1). In this study, the three ensembles, r1i1p1, r2i1p1, and r3i1p1, were randomly selected which are commonly available for the selected GCMs and RCPs. For the GCMs with different spatial resolutions, a common resolution can be obtained through regridding or downscaling (Zarekarizi et al., 2018). In this study, the GCM projections were regridded to a

Table 1
Summary of Daily Precipitation Projections From the CMIP5 Depository Used in This Study

GCM	Institution	Reference	Resolution (Lat × Lon in °)
CanESM2	Canadian Centre for Climate Modelling and Analysis	Chylek et al. (2011)	2.7906 × 2.8125
CSIRO-MK3–6-0	Australian Commonwealth Scientific and Industrial Research Organization (CSIRO) Marine and Atmospheric Research in collaboration with the Queensland Climate Change Centre of Excellence (QCCCE)	Gordon et al. (2002)	1.8653 × 1.875
HadGEM2-ES	Met Office Hadley Centre, UK	*C* Jones et al. (2011)	1.25 × 1.875
IPSL-CM5A-LR	Institut Pierre Simon Laplace, France	Dufresne et al. (2013)	1.8947 × 3.75
MIROC5	Atmosphere and Ocean Research Institute, The University of Tokyo, Japan	Watanabe et al. (2010)	1.4008 × 1.40625

resolution of 2.5° × 2.5° through the second-order spline interpolation which is known as appropriate for flux variables such as precipitation (Herold et al., 2017; P. W. Jones, 1999).

2.2. SREV

We quantify the uncertainty in precipitation projections using the square root of error variance (SREV) metric, introduced by F. M. Woldemeskel et al. (2012) to estimate monthly temperature and precipitation uncertainties using the CMIP3 future climate projections. This assessment was later extended in F. M. Woldemeskel et al. (2016) to monthly precipitation and temperature from CMIP5 projections, showing a general reduction in model structural uncertainty through the use of newer generation models. SREV indicates the uncertainty in an estimated climate variable by calculating the spread of projections around its mean. The derivation of SREV and associated equations are provided by F. M. Woldemeskel et al. (2012), and further explained in S. Eghdamirad et al. (2016); F. M. Woldemeskel et al. (2014); F. M. Woldemeskel et al. (2016). Here, we briefly review the method for estimating SREV.

The first step is to convert data to percentiles at each grid cell. By doing so, deviations across each simulation can be established in percentile (e.g., 99th percentile) space. The second step is to estimate SREV for a percentile of interest as the standard deviation of all projections. This is to individually estimate model, scenario, and ensemble uncertainties. If needed, the estimated SREV for each percentile is recast as a time series, as each. Here, Equations 1 to 3 are used to calculate the model (M), scenario (S), and ensemble (E) uncertainties at each percentile (p), denoted as SREV_p^M, SREV_p^S, and SREV_p^E, respectively.

$$\mathrm{SREV}_p^M = \left[\frac{1}{n_S n_E (n_M - 1)} \sum_{j=1}^{n_S} \sum_{k=1}^{n_E} \sum_{i=1}^{n_M} \left(x_{i,j,k,p} - \overline{x}_{j,k,p}\right)^2\right]^{0.5} \tag{1}$$

$$\mathrm{SREV}_p^S = \left[\frac{1}{n_E n_M (n_S - 1)} \sum_{k=1}^{n_E} \sum_{i=1}^{n_M} \sum_{j=1}^{n_S} \left(x_{i,j,k,p} - \overline{x}_{k,i,p}\right)^2\right]^{0.5} \tag{2}$$

$$\mathrm{SREV}_p^E = \left[\frac{1}{n_M n_S (n_E - 1)} \sum_{i=1}^{n_M} \sum_{j=1}^{n_S} \sum_{k=1}^{n_E} \left(x_{i,j,k,p} - \overline{x}_{i,j,p}\right)^2\right]^{0.5} \tag{3}$$

where the number of models, scenarios, and ensembles are denoted as n_M, n_S, and n_E, respectively. $x_{i,j,k,p}$ is the pth percentile of a projection using the ith model, jth scenario, and kth ensemble. $\overline{x}_{j,k,p}$, $\overline{x}_{k,i,p}$, and $\overline{x}_{i,j,p}$ are the mean of the values over all models, scenarios, and ensembles at the percentile, respectively.

This process is undertaken at each p for each source of uncertainty. Then the total uncertainty (SREV_p^T) is calculated as the square root of the sum of the squares of individual SREV components as

$$\mathrm{SREV}_p^T = \left[\left(\mathrm{SREV}_p^M\right)^2 + \left(\mathrm{SREV}_p^S\right)^2 + \left(\mathrm{SREV}_p^E\right)^2\right]^{0.5} \tag{4}$$

The unit for the SREV is identical to that of precipitation (i.e., "mm") and the SREV is regarded to the conditional total standard deviation of the variable of interest at a percentile, and therefore the SREV can be used for stating uncertainty of the GCM outputs (F. M. Woldemeskel et al., 2012). Once calculated, the

final step entails transferring the estimated SREV to the original time-space by adopting the value corresponding to the percentile the simulation represents. In other words, each time step in the GCM simulation is converted to an equivalent percentile, and then the SREV associated with that percentile used to express its associated uncertainty. This SREV method is based on assuming that the GCMs used in the analysis are independent of each other with consistent nonexceedance probabilities and equal uncertainty at any percentile (F. M. Woldemeskel et al., 2012). More importantly, even though the SREV calculation using Equation 4 is based on assuming that there is no interaction between the three terms of uncertainty (Hawkins & Sutton, 2009), this simplification is controversial and this point is further discussed in section 3.3.

As the SREV is considered as the conditional total standard deviation around the mean for any percentile, finally, a relative SREV was calculated for the result presentation, which, similar to the coefficient of variation (CV), is formed by dividing the SREV by the mean of all projections at that percentile. This process not only helps to compare uncertainty at different percentiles for the same grid point but also assists in comparing uncertainties across different grid points. When using simulations in water resources management, the relative SREV is more important than its absolute value. To emphasize the importance of relative SREV, for example, one can compare two regions, Southeast Asia and the Middle East. In the former, an uncertainty of 20 mm in annual precipitation may represent 0.5% of the total mean annual precipitation. On the other hand, an uncertainty of 20 mm in mean annual precipitation of some regions in the Middle East exceeds 10% of annual precipitation, which could have a large impact on planning for human activities.

3. Results and Discussion

Uncertainty in daily extreme precipitation is calculated across the globe for simulations of the 21st century (2006–2100). The uncertainty has been decomposed into its three sources to illustrate the influence of each source on total uncertainty in future daily precipitation projections. Note that the results for mean precipitation are presented in the supporting information for comparisons.

3.1. Relative SREV by Region

As shown in Figure 1, the uncertainty in precipitation was calculated for four precipitation exceedance thresholds of 100th, 99.9th, 99.0th, and 95.0th percentiles as adopted by existing studies for extreme precipitation (Herold et al., 2017; Westra et al., 2014). The left-hand column in Figure 1 shows the mean values of the precipitation more than the percentiles, and the right column shows the associated relative SREV. For example, the maximum daily precipitation for each of the 45 projections was represented as the 100th percentile. For each projection, the selected value is the maximum projected daily precipitation value during the 95-year simulation period (2006–2100). Then, the mean of the 45 maximum values (Figure 1a) and the relative SREV for those values (Figure 1b) were calculated.

According to the left-hand column of Figure 1, the spatial distribution of extreme precipitation for the four exceedance thresholds generally remains consistent at the global scale with some changes at the regional scale. For example, Figure 1a shows that the very north of Australia has almost the same maximum rainfall as Southeast Asia. On the other hand, Figure 1g shows that the 95th percentile rainfall in northern Australia and Southeast Asia are considerably different. The relative SREV in extreme precipitation is shown in the right-hand column of Figure 1. Compared to the case of mean precipitation (Figure S1c in the supporting information), there is greater spatial difference in the relative SREV calculated for extreme precipitation and the highest relative SREV is presented for the case with maximum precipitation values.

As shown in Figure 2, the results presented in Figure 1 are regionally aggregated to the 22 land regions as suggested by Giorgi and Francisco (2000). The regions on the horizontal axis are sorted by the regionally averaged mean relative SREV. The right axis shows regional mean daily precipitation, and the left axis shows the average relative SREV for each region.

Figure 2 shows that the relative SREV in precipitation projections is not so relevant to the amounts of mean precipitation. For example, the Sahara is the driest region and has the highest relative SREV. However, Central Asia is also a dry region but has medium relative SREV. Furthermore, Southeast Asia, the wettest region, has moderately low relative SREV. It can be concluded that relative agreement or disagreement among models on modeling precipitation does not depend on the regional amounts of mean precipitation. One should, however, note that the absolute uncertainty as expressed by the SREV (and not the relative

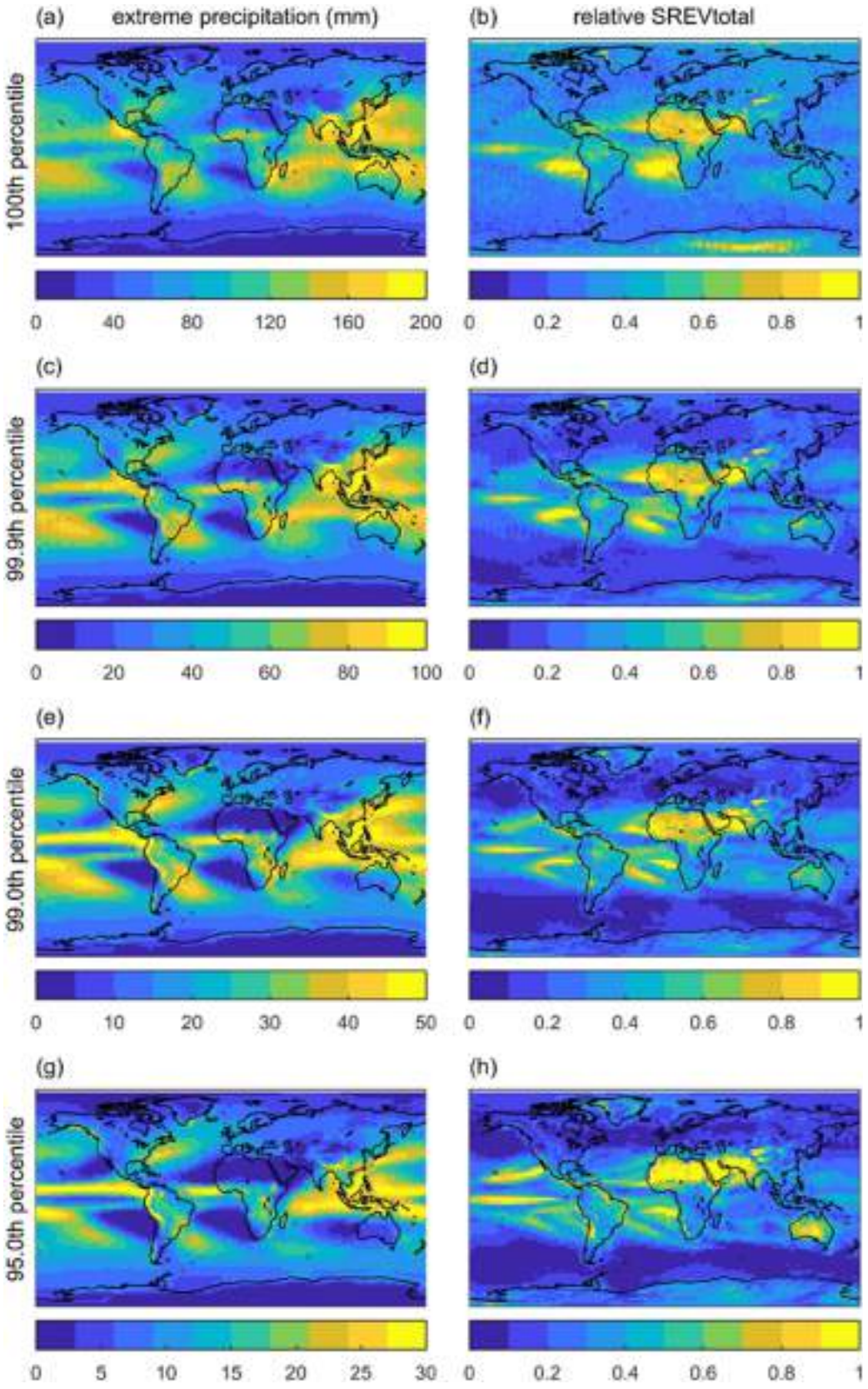

Figure 1. Spatial distribution of daily precipitation extremes and their relative SREVs over the period 2006–2100 for 45 projections. The left column (a, c, e, g) shows the average of an exceedance threshold value, the right column (b, d, f, h) shows the relative total SREV.

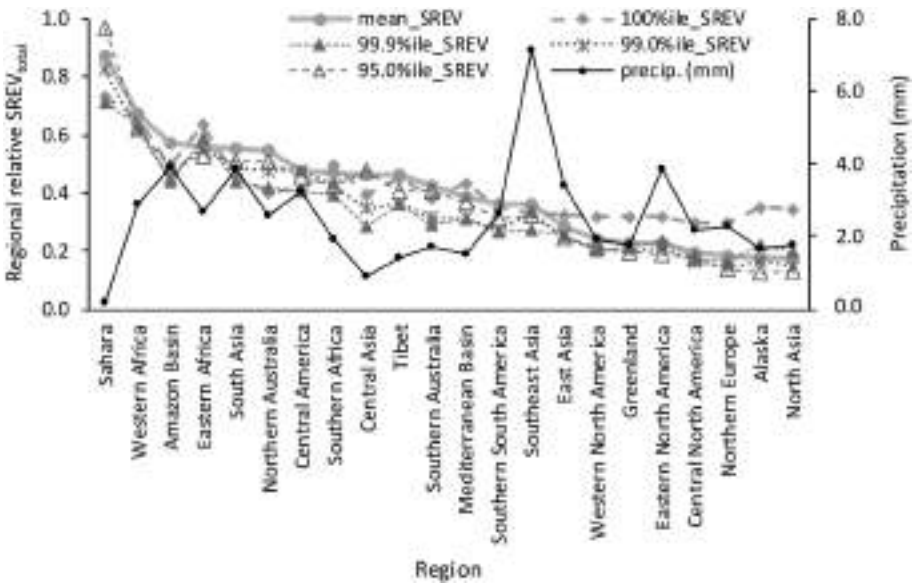

Figure 2. Regional average of mean precipitation (right axis) and relative total uncertainty of extremes (left axis) for 45 projections of daily precipitation over the period 2006–2100.

SREV) is generally greater for higher precipitation regions, consistent with previous studies that have focused on this issue(F. Woldemeskel & Sharma, 2016).

Figure 2 shows that the relative SREV strongly depends on the region. This means that if a region has high, medium, or low relative SREV for projections of mean precipitation, then the uncertainty in extreme precipitation projections is also predominantly high, medium, or low, respectively. In all northern regions of the Northern Hemisphere (including Alaska, western North America, central North America, eastern North America, Greenland, Northern Europe, and North Asia), a different pattern of relative SREV is observed for the maximum precipitation. In these regions, while the relative SREV is similar for 95.0th–99.9th percentile extreme precipitation and mean precipitation, the relative SREV of the maximum precipitation is noticeably higher. This finding is consistent with other studies which demonstrated that GCMs might exhibit markedly different skills in modeling mean and extreme precipitation (in this case the maximum of extremes) because of changes in the water-holding capacity of warmer air (Fischer & Knutti, 2015).

3.2. SREV Components by Source

The spatial distribution of the three sources of uncertainty for extreme precipitation is shown in Figures 3 and 4 where regions are sorted by their amounts of mean precipitation (Southeast Asia is the wettest, and the Sahara is the driest).

As shown in Figures 3b and 3c, it is notable that scenario and ensemble uncertainties are higher compared to the other exceedance thresholds for the maximum percentile precipitation. For the maximum percentile extremes, ensemble uncertainty is as high as scenario uncertainty, unlike the results for the lower extremes (i.e., 99.9th, 99.0th, and 95.0th percentiles), where scenario uncertainty is noticeably higher. This indicates that there is considerably greater disagreement between GCM results for the maximum precipitation than for the more frequent extreme values.

Figure 4 shows the regionally aggregated results from Figure 3.

According to Figure 4, in some regions, the relative model SREV in the maximum percentile is less than those of the other percentiles. This difference is commonly observed in the driest (the Sahara) and wettest (Southeast Asia) regions. As the total uncertainty is the square root of the sum of the squares of the individual SREV components presented in Equation 4, when the scenario and ensemble components are considerably smaller than the model component (e.g., the 99.9th, 99.0th, and 95.0th percentile in Figures 4b–4d), the total uncertainty is very close to the dominant component, model uncertainty. On the other hand, for the

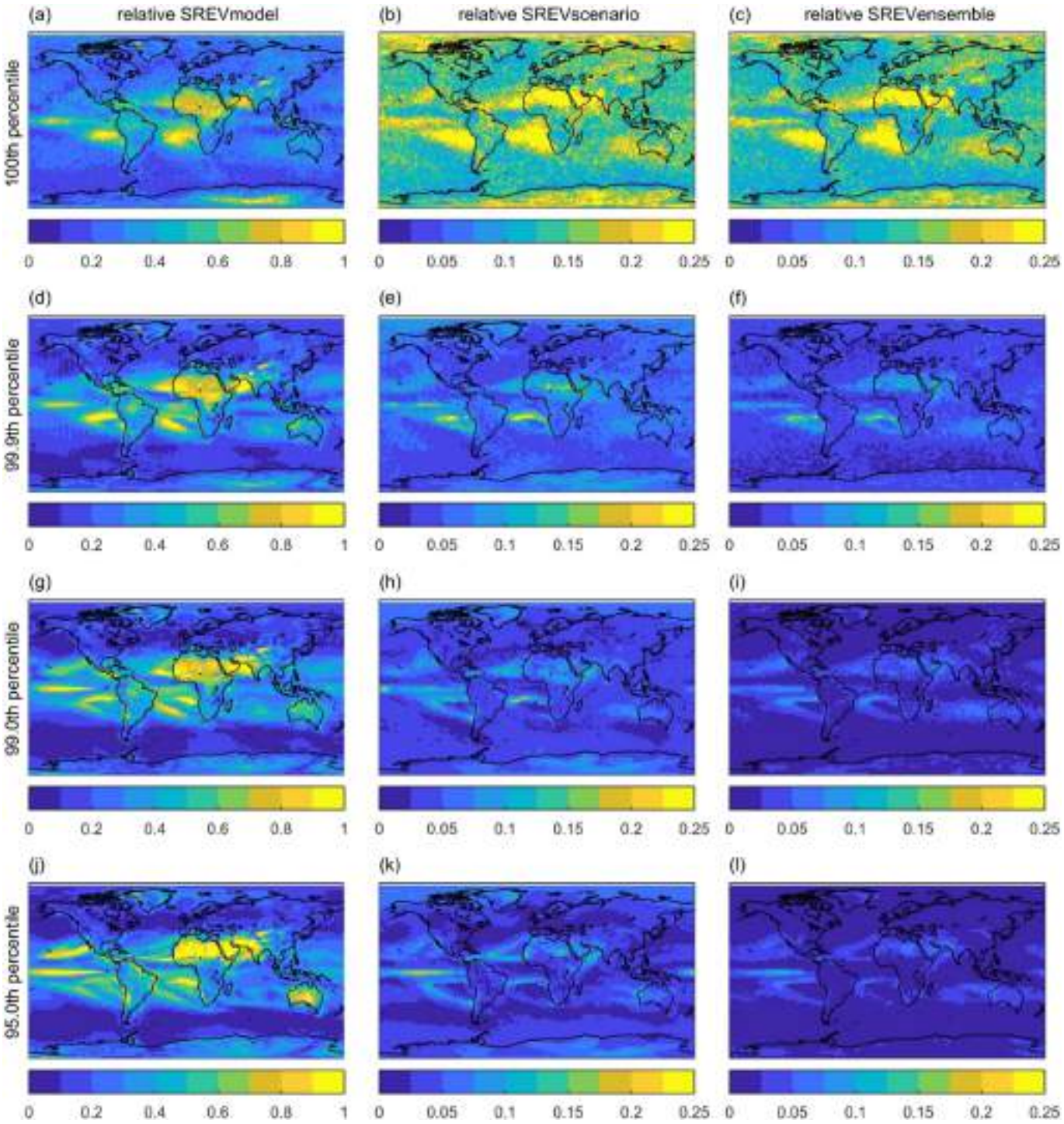

Figure 3. Spatial distribution of the three sources of uncertainty for extreme precipitation over the period 2006–2100. The left column (a, d, g, j) shows the relative SREV by model for 100th, 99.9th, 99.0th and 95.0th percentiles, respectively; the middle column (b, e, h, k) for the relative SREV by scenario; the right column (c, f, i, l) for the relative SREV by ensemble.

maximum percentile extremes, due to the contribution of scenario and ensemble uncertainties, total uncertainty is clearly higher than model uncertainty.

The percentage contributions of the three sources of relative SREV for extreme precipitation are shown in Figure 5 for different regions across the globe.

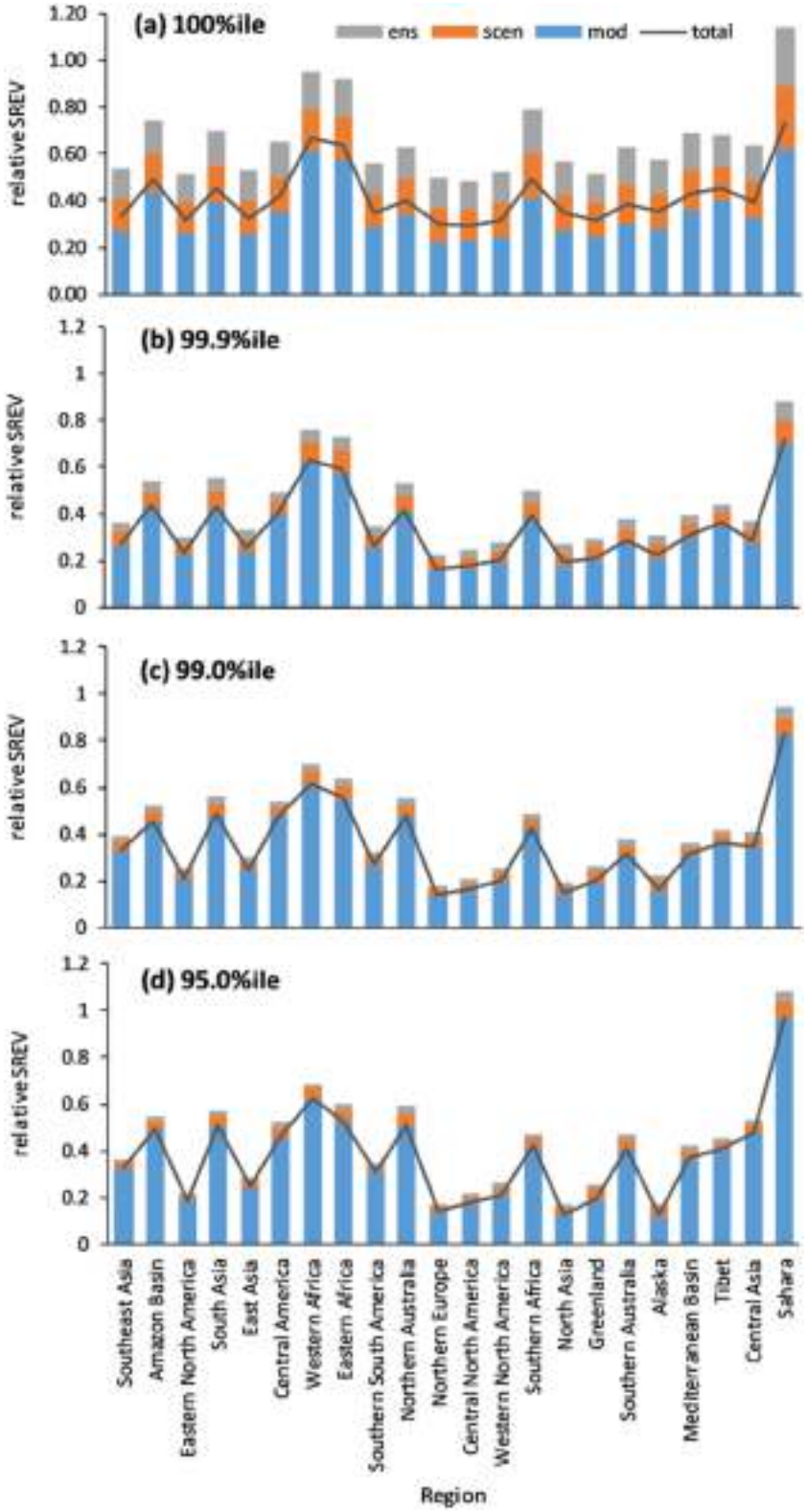

Figure 4. Regionally aggregated relative SREV for total uncertainty and three sources of uncertainty over the period 2006–2100, for (a)100th percentile, (b)99.9th percentile, (c)99.0th percentile and (d)95.0th percentile.

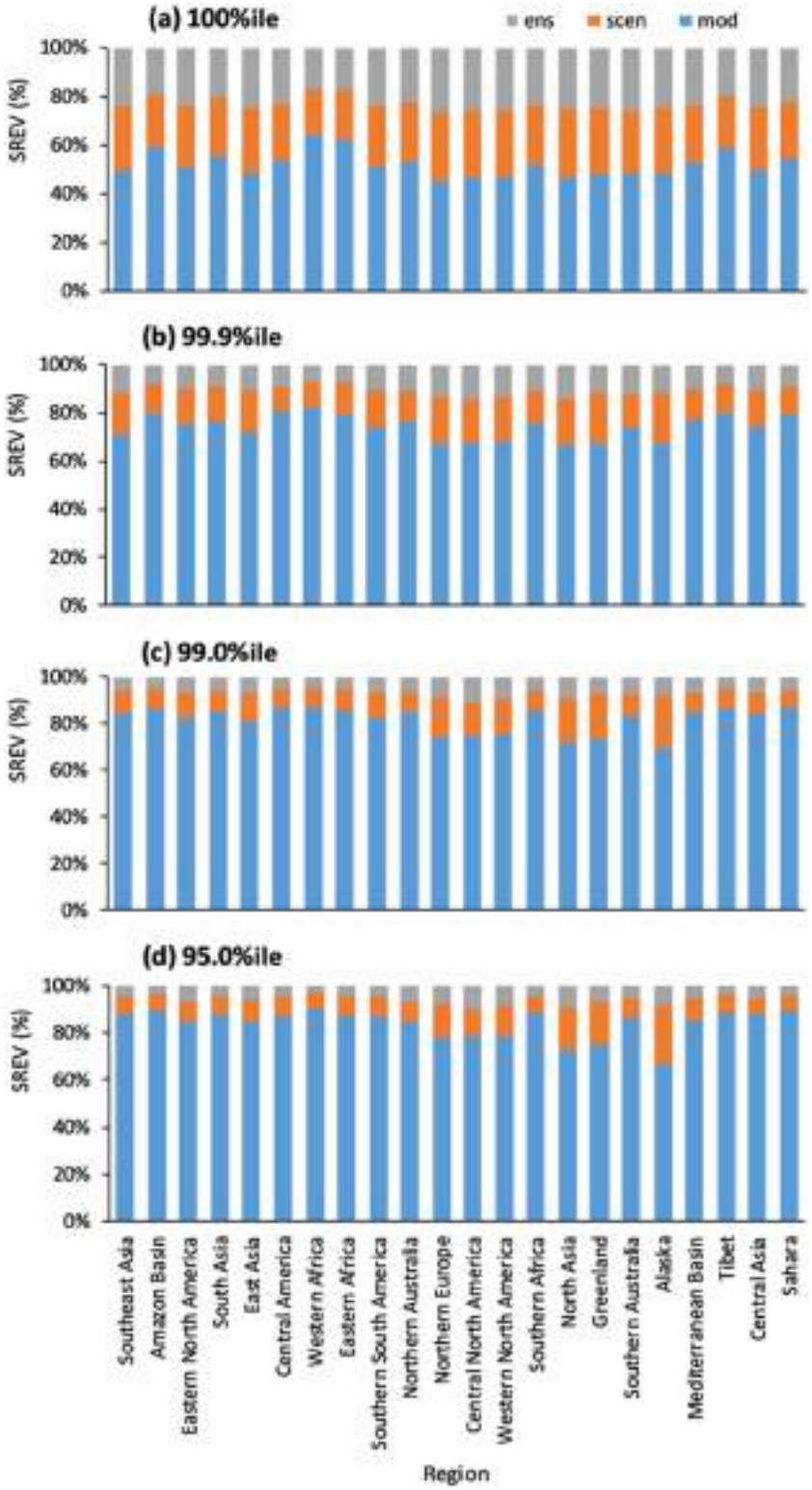

Figure 5. Contribution of the three sources of relative SREV for extreme precipitation over the period 2006–2100 for each region, for (a)100th percentile, (b)99.9th percentile, (c)99.0th percentile and (d)95.0th percentile.

The influence of scenario and ensemble uncertainties decreases from the maximum percentile to the lower percentiles. The ensemble uncertainty is only as significant as the scenario uncertainty for the maximum percentile extreme precipitation. In Alaska, Greenland, and North Asia, the disagreement between the climate models regarding the climate scenarios (i.e., scenario uncertainty) is significantly higher than the ensemble uncertainty. To a lower extent, this result is also observed in Northern Europe, western North America, central North America, and eastern North America. This finding indicates that higher total uncertainty in the maximum percentile results for the northern part of the Northern Hemisphere (Figure 2) may originate from higher ensemble uncertainty.

3.3. Caveats and Future Works

There are some discussion points which are worth investigating in future studies. First, an assumption in the SREV calculation presented here is that there is no interaction between the three sources of uncertainty (Hawkins & Sutton, 2009, 2011; F. M. Woldemeskel et al., 2012; F. M. Woldemeskel et al., 2014). However, it is necessary for this to be further considered for better assessments of reliability. Van Uytven and Willems (2018) assessed the contribution of the interaction of greenhouse gas scenario and climate model uncertainty to the total variance of the changes in daily precipitation projections for central Belgium and presented that the interaction term is identified as a unignorable uncertainty source. Yip et al. (2011) also showed that this assumption may not always hold and that interactions between the model and scenario uncertainties could be important. S. Eghdamirad et al. (2016) found that the interaction term for the different climate variables varies between 13% and 23% through a test using climate variables at a single grid point over multiple projections. The assumption of independence hence needs further investigation in terms of interpreting results and improving the SREV concept, which can be addressed through further development.

Second, from this study, it was concluded that the model uncertainty is the major contributor to the total uncertainty, followed by the scenario and ensemble uncertainties. Even though F. M. Woldemeskel et al. (2016) and S. Eghdamirad et al. (2016) have shown that bias correction can significantly reduce model uncertainty, in this study, the original precipitation projections were used without any correction to avoid the additional uncertainty of bias correction in regard to extreme precipitation (Evans & Argüeso, 2014). It should be noted that depending on the type of bias correction, the findings may change in terms of the model uncertainty. However, the results for the scenario and ensemble uncertainties might not be expected to change.

Third, given that uncertainty analysis for flood events depends on both depth and temporal pattern of heavy precipitation (C. Wasko & Sharma, 2015), in this study, the uncertainty in extreme daily precipitation was investigated only for the depth of 1-day precipitation. This study could be further developed to reveal how uncertainty in extreme precipitation changes with respect to the storm period and temporal storm patterns. In addition, the results of this study should be investigated separately for different seasons to assist in water policy and planning in regions with significant seasonal storage requirements. Moreover, the results are expected to change regionally and globally if the simulations are temporally extended or reduced, due to the nonmonotonic behavior of precipitation over time (Hawkins et al., 2014).

Fourth, it is worthwhile to implement the proposed SREV analysis with different models, RCPs, and ensembles. Hosseinzadehtalaei et al. (2017) concluded through sensitivity analyses that the GCM, RCP, and GCM initial condition uncertainties are greatly influenced by the set of climate model runs considered, especially for more extreme precipitation at finer time scales, and ensemble sizes. It should be also noted that the SREV method can be extended with more categories (e.g., grouping models by physical basis) by which a detailed understanding on the uncertainty can be obtained.

Fifth, although this study focused on presenting the regional differences with temporally aggregated SREV time series, it is also necessary to investigate how the SREV varies with time. As the relative importance of the different components of uncertainty varies with time (Hawkins & Sutton, 2011), the SREV time series might provide additional insights that could enhance the reported results.

Sixth, a key advantage of the proposed approach is the ability to quantify uncertainty in a sequence of precipitation days. While the focus here has been on a specific percentile, given the impact the uncertainty specification for, say, a design storm, this issue needs further assessment. Additionally, how much of this

uncertainty present in such a design storm event translates into a derived flood or volume is an additional factor that needs documentation.

Lastly, the proposed method can be applied for any multiple products including historical data sets derived from various models and conditions, it is worthwhile to assess uncertainties of such data sets through the proposed methodology. Especially, as the CMIP6 data sets are now operationally available (Eyring et al., 2016), it would be beneficial to apply the SREV method for an insight into the uncertainty in the CMIP6 outcomes.

4. Summary and Conclusions

This study focused on uncertainty in daily precipitation projections for a 95-year period (2006–2100) by quantifying the disagreement among GCM results. Three sources of uncertainty were considered: model, scenario, and ensemble uncertainties and was quantified at a daily time scale for 45 global precipitation projections from five GCMs, three RCPs, and three ensembles using the percentile-based SREV concept.

It has been generally acknowledged that the largest change in future precipitation may occur in wet regions, with higher expected precipitation (Fischer & Knutti, 2015). Based on the findings of this study, it was concluded that the relative SREV in precipitation projections strongly depends on the region, but not necessarily on the amount of regional precipitation. An issue identified here is that there is high relative SREV (disagreement between models) in dry regions such as the Middle East, North Africa, and some parts of Australia. This means our understanding of future precipitation is more uncertain in dry regions compared to wet regions, of added concern given the changes expected ahead (Asadi Zarch et al., 2015). In addition to this, it was also revealed that the total relative SREV and its components show different spatial distributions across the globe. Furthermore, the uncertainty in extreme precipitation projections was investigated for four thresholds of 100th, 99.9th, 99.0th, and 95.0th percentiles. At the regional scale, the relative SREV in daily precipitation did not differ noticeably for extreme projections. Also, it was shown that climate scenarios and ensembles have a strong influence on the uncertainty in the extreme precipitation projections.

This study presented a basis to compare uncertainty in future projections of daily extreme precipitation. Clarifying uncertainty in climate projections is important for policymakers' perception of climate change (McMahon et al., 2015). This paper makes some meaningful steps toward assisting in quantifying the influence of climate on habitability (Marotzke et al., 2017), enabling policymakers and water authorities to adopt future water policies and plans with explicit consideration of uncertainty at the catchment scale. The authors also hope that the results presented here could provide some guidelines for researchers.

Data Availability Statements

The Coupled Model Intercomparison Project Phase 5 (CMIP5) data repository is freely available at https://esgf-node.llnl.gov/projects/cmip5/, where the 45 projections used in this study can be searched by the five GCMs (i.e., CanESM2, CSIRO-MK3-6-0, HadGEM2-ES, IPSL-CM5A-LR, and MIROC5), the three scenarios (RCP2.6, RCP4.5, and RCP8.5) and the three ensembles (r1i1p1, r2i1p1, and r3i1p1).

Acknowledgments

This work was supported by the National Research Foundation of Korea (NRF) under a Grant funded by the Korean government (MSIP) (NRF-2019R1A2B5B03069810). We acknowledge the World Climate Research Programme's Working Group on Coupled Modeling, which is responsible for CMIP, and we thank the climate modeling groups for producing and making their model output available. For CMIP, the U.S. Department of Energy's Program for Climate Model Diagnosis and Intercomparison provides coordinating support and led the development of software infrastructure in partnership with the Global Organization for Earth System Science Portals.

References

Alexander, K., Hettiarachchi, S., Ou, Y., & Sharma, A. (2019). Can integrated green spaces and storage facilities absorb the increased risk of flooding due to climate change in developed urban environments? *Journal of Hydrology*, *579*, 124,201.

Alexander, L. V., & Arblaster, J. M. (2017). Historical and projected trends in temperature and precipitation extremes in Australia in observations and CMIP5. *Weather and Climate Extremes*, *15*, 34–56.

Asadi Zarch, M. A., Sivakumar, B., & Sharma, A. (2015). Assessment of global aridity change. *Journal of Hydrology*, *520*, 300–313. https://doi.org/10.1016/j.jhydrol.2014.11.033

Chylek, P., Li, J., Dubey, M., Wang, M., & Lesins, G. (2011). Observed and model simulated 20th century Arctic temperature variability: Canadian earth system model CanESM2. *Atmospheric Chemistry and Physics Discussions*, *11*, 22,893–22,907.

Deser, C., Knutti, R., Solomon, S., & Phillips, A. S. (2012). Communication of the role of natural variability in future North American climate. *Nature Climate Change*, *2*, 775–779.

Dufresne, J.-L., Foujols, M.-A., Denvil, S., Caubel, A., Marti, O., Aumont, O., et al. (2013). Climate change projections using the IPSL-CM5 earth system model: From CMIP3 to CMIP5. *Clim Dynam*, *40*, 2123–2165.

Eghdamirad, S., Johnson, F., & Sharma, A. (2017). How reliable are GCM simulations for different atmospheric variables? *Climatic Change*, *145*, 237–248. https://doi.org/10.1007/s10584-017-2086-x

Eghdamirad, S., Johnson, F., Woldemeskel, F., & Sharma, A. (2016). Quantifying the sources of uncertainty in upper air climate variables. *Journal of Geophysical Research: Atmospheres*, *121*, 3859–3874. https://doi.org/10.1002/2015JD024341

Evans, J. P., & Argüeso, D. (2014). *Guidance on the use of bias corrected data. NARCliM Technical Note 3* (pp. 1–7). Sydney, Australia: NARCliM consortium.
Eyring, V., Bony, S., Meehl, G. A., Senior, C. A., Stevens, B., Stouffer, R. J., & Taylor, K. E. (2016). Overview of the Coupled Model Intercomparison Project Phase 6 (CMIP6) experimental design and organization. *Geoscientific Model Development*, *9*, 1937–1958.
Fischer, E. M., Beyerle, U., & Knutti, R. (2013). Robust spatially aggregated projections of climate extremes. *Nature Climate Change*, *3*, 1033–1038. https://doi.org/10.1038/nclimate2051
Fischer, E. M., & Knutti, R. (2015). Anthropogenic contribution to global occurrence of heavy-precipitation and high-temperature extremes. *Nature Climate Change*, *5*, 560–564. https://doi.org/10.1038/nclimate2617
Fischer, E. M., Sedláček, J., Hawkins, E., & Knutti, R. (2014). Models agree on forced response pattern of precipitation and temperature extremes. *Geophysical Research Letters*, *41*, 8554–8562. https://doi.org/10.1002/2014gl062018
Giorgi, F., & Francisco, R. (2000). Uncertainties in regional climate change prediction: A regional analysis of ensemble simulations with the HADCM2 coupled AOGCM. *Clim Dynam*, *16*(2–3), 169–182.
Gordon, H. B., Rotstayn, L. D., McGregor, J. L., Dix, M. R., Kowalczyk, E. A., O'Farrell, S. P., et al. (2002). *The CSIRO Mk3 climate system model*. Victoria, Australia: CSIRO Atmospheric Research.
Hawkins, E., Joshi, M., & Frame, D. (2014). Wetter then drier in some tropical areas. *Nature Climate Change*, *4*, 646–647. https://doi.org/10.1038/nclimate2299
Hawkins, E., & Sutton, R. (2009). The potential to narrow uncertainty in regional climate predictions. *Bulletin of the American Meteorological Society*, *90*, 1095–1107. https://doi.org/10.1175/2009bams2607.1
Hawkins, E., & Sutton, R. (2011). The potential to narrow uncertainty in projections of regional precipitation change. *Clim Dynam*, *37*, 407–418.
Hayhoe, K., Wake, C. P., Huntington, T. G., Luo, L., Schwartz, M. D., Sheffield, J., et al. (2007). Past and future changes in climate and hydrological indicators in the US northeast. *Clim Dynam*, *28*, 381–407.
Hegerl, G. C., Black, E., Allan, R. P., Ingram, W. J., Polson, D., Trenberth, K. E., et al. (2015). Challenges in quantifying changes in the global water cycle. *Bulletin of the American Meteorological Society*, *96*, 1097–1115. https://doi.org/10.1175/bams-d-13-00212.1
Herold, N., Behrangi, A., & Alexander, L. V. (2017). Large uncertainties in observed daily precipitation extremes over land. *Journal of Geophysical Research: Atmospheres*, *122*, 668–681. https://doi.org/10.1002/2016JD025842
Hettiarachchi, S., Wasko, C., & Sharma, A. (2018). Increase in flood risk resulting from climate change in a developed urban watershed—The role of storm temporal patterns. *Hydrology and Earth System Sciences*, *22*, 2041–2056. https://doi.org/10.5194/hess-22-2041-2018
Hettiarachchi, S., Wasko, C., & Sharma, A. (2019). Can antecedent moisture conditions modulate the increase in flood risk due to climate change in urban catchments? *Journal of Hydrology*, *571*, 11–20.
Hosseinzadehtalaei, P., Tabari, H., & Willems, P. (2017). Uncertainty assessment for climate change impact on intense precipitation: How many model runs do we need? *International Journal of Climatology*, *37*, 1105–1117.
IPCC (2014). *Climate change 2013: The physical science basis: Working group I contribution to the fifth assessment report of the Intergovernmental Panel on Climate Change*. Cambridge, United Kingdom and New York, NY, USA: Cambridge University Press. https://doi.org/10.1017/CBO9781107415324
Jones, C., Hughes, J., Bellouin, N., Hardiman, S., Jones, G., Knight, J., et al. (2011). The HadGEM2-ES implementation of CMIP5 centennial simulations. *Geoscientific Model Development*, *4*, 543–570.
Jones, P. W. (1999). First-and second-order conservative remapping schemes for grids in spherical coordinates. *Monthly Weather Review*, *127*(9), 2204–2210.
Kharin, V. V., Zwiers, F. W., Zhang, X., & Wehner, M. (2013). Changes in temperature and precipitation extremes in the CMIP5 ensemble. *Climatic Change*, *119*, 345–357. https://doi.org/10.1007/s10584-013-0705-8
Kundzewicz, Z. W., Mata, L., Arnell, N. W., Döll, P., Jimenez, B., Miller, K., et al. (2008). The implications of projected climate change for freshwater resources and their management. *Hydrological Sciences Journal*, *53*, 3–10.
Marotzke, J., Jakob, C., Bony, S., Dirmeyer, P. A., O'Gorman, P. A., Hawkins, E., et al. (2017). Climate research must sharpen its view. *Nature Climate Change*, *7*, 89–91. https://doi.org/10.1038/nclimate3206
McMahon, R., Stauffacher, M., & Knutti, R. (2015). The unseen uncertainties in climate change: Reviewing comprehension of an IPCC scenario graph. *Climatic Change*, *133*, 141–154. https://doi.org/10.1007/s10584-015-1473-4
Meinshausen, M., Meinshausen, N., Hare, W., Raper, S. C., Frieler, K., Knutti, R., et al. (2009). Greenhouse-gas emission targets for limiting global warming to 2°C. *Nature*, *458*, 1158–1162. https://doi.org/10.1038/nature08017
Meinshausen, M., Smith, S. J., Calvin, K., Daniel, J. S., Kainuma, M., Lamarque, J.-F., et al. (2011). The RCP greenhouse gas concentrations and their extensions from 1765 to 2300. *Climatic Change*, *109*, 213.
Miller, K. A., & D. N. Yates (2006). Climate change and water resources: A primer for municipal water providers, American Water Works Association.
Murphy, J. M., Sexton, D. M., Barnett, D. N., Jones, G. S., Webb, M. J., Collins, M., & Stainforth, D. A. (2004). Quantification of modelling uncertainties in a large ensemble of climate change simulations. *Nature*, *430*, 768–772. https://doi.org/10.1038/nature02771
Peters, G. P., Andrew, R. M., Boden, T., Canadell, J. G., Ciais, P., Le Quéré, C., et al. (2012). The challenge to keep global warming below 2°C. *Nature Climate Change*, *3*, 4.
Randall, D. A., Wood, R. A., Bony, S., Colman, R., Fichefet, T., Fyfe, J., et al. (2007). climate models and their evaluation, in *Climate change 2007: The physical science basis. Contribution of Working Group I to the Fourth Assessment Report of the IPCC (FAR)*, edited (pp. 589-662). Cambridge, United Kingdom and New York, NY, USA: Cambridge University Press.
Schleussner, C.-F., Rogelj, J., Schaeffer, M., Lissner, T., Licker, R., Fischer, E. M., et al. (2016). Science and policy characteristics of the Paris agreement temperature goal. *Nature Climate Change*, *6*, 827.
Sharma, A., Wasko, C., & Lettenmaier, D. P. (2018). If precipitation extremes are increasing, why aren't floods? *Water Resources Research*, *54*, 8545–8551. https://doi.org/10.1029/2018wr023749
Sillmann, J., Kharin, V. V., Zwiers, F. W., Zhang, X., & Bronaugh, D. (2013). Climate extremes indices in the CMIP5 multimodel ensemble: Part 2. Future climate projections. *Journal of Geophysical Research: Atmospheres*, *118*, 2473–2493. https://doi.org/10.1002/jgrd.50188
Stainforth, D. A., Aina, T., Christensen, C., Collins, M., Faull, N., Frame, D. J., et al. (2005). Uncertainty in predictions of the climate response to rising levels of greenhouse gases. *Nature*, *433*, 403.
Teng, J., Vaze, J., Chiew, F. H., Wang, B., & Perraud, J.-M. (2012). Estimating the relative uncertainties sourced from GCMs and hydrological models in modeling climate change impact on runoff. *Journal of Hydrometeorology*, *13*, 122–139.
Van Uytven, E., & Willems, P. (2018). Greenhouse gas scenario sensitivity and uncertainties in precipitation projections for central Belgium. *Journal of Hydrology*, *558*, 9–19. https://doi.org/10.1016/j.jhydrol.2018.01.018

Van Vuuren, D. P., Edmonds, J., Kainuma, M., Riahi, K., Thomson, A., Hibbard, K., et al. (2011). The representative concentration pathways: An overview. *Climatic Change*, *109*, 5–31.

Vermeulen, S. J., Campbell, B. M., & Ingram, J. S. (2012). Climate change and food systems. *Annual Review of Environment and Resources*, *37*, 195–222.

Wasko, C., & Sharma, A. (2015). Steeper temporal distribution of rain intensity at higher temperatures within Australian storms. *Nature Geoscience*, *8*, 527–529. https://doi.org/10.1038/Ngeo2456

Wasko, C., Sharma, A., & Johnson, F. (2015). Does storm duration modulate the extreme precipitation-temperature scaling relationship? *Geophysical Research Letters*, *42*, 8783–8790. https://doi.org/10.1002/2015GL066274

Watanabe, M., Suzuki, T., O'ishi, R., Komuro, Y., Watanabe, S., Emori, S., et al. (2010). Improved climate simulation by MIROC5: Mean states, variability, and climate sensitivity. *Journal of Climate*, *23*, 6312–6335.

Westra, S., Fowler, H. J., Evans, J. P., Alexander, L. V., Berg, P., Johnson, F., et al. (2014). Future changes to the intensity and frequency of short-duration extreme rainfall. *Reviews of Geophysics*, *52*, 522–555. https://doi.org/10.1002/2014rg000464

Woldemeskel, F., & Sharma, A. (2016). Should flood regimes change in a warming climate? The role of antecedent moisture conditions. *Geophysical Research Letters*, *43*, 7556–7563.

Woldemeskel, F. M., Sharma, A., Sivakumar, B., & Mehrotra, R. (2012). An error estimation method for precipitation and temperature projections for future climates, *Journal of Geophysical Research: Atmospheres*, *117*(D22104), 1–13. https://doi.org/10.1029/2012JD018062

Woldemeskel, F. M., Sharma, A., Sivakumar, B., & Mehrotra, R. (2014). A framework to quantify GCM uncertainties for use in impact assessment studies. *Journal of Hydrology*, *519*, 1453–1465. https://doi.org/10.1016/j.jhydrol.2014.09.025

Woldemeskel, F. M., Sharma, A., Sivakumar, B., & Mehrotra, R. (2016). Quantification of precipitation and temperature uncertainties simulated by CMIP3 and CMIP5 models. *Journal of Geophysical Research: Atmospheres*, *121*, 3–17. https://doi.org/10.1002/2015JD023719

Xie, S.-P., Deser, C., Vecchi, G. A., Collins, M., Delworth, T. L., Hall, A., et al. (2015). Towards predictive understanding of regional climate change. *Nature Climate Change*, *5*, 921–930. https://doi.org/10.1038/nclimate2689

Yip, S., Ferro, C. A. T., Stephenson, D. B., & Hawkins, E. (2011). A simple, coherent framework for partitioning uncertainty in climate predictions. *Journal of Climate*, *24*, 4634–4643. https://doi.org/10.1175/2011jcli4085.1

Zarekarizi, M., Rana, A., & Moradkhani, H. (2018). Precipitation extremes and their relation to climatic indices in the Pacific Northwest USA. *Clim Dynam*, *50*, 4519–4537.